The Onset of Orientational Crystallization in Poly(ethylene terephthalate) During Low Temperature Drawing

C. M. ROLAND *and* M. F. SONNENSCHEIN*

Chemistry Division, Code 6120
Naval Research Laboratory
Washington, D.C. 20375-5000

It is well known that crystallization can be induced in amorphous poly(ethylene terephthalate) (PET) by orientation below the isotropic crystallization temperature. The magnitude of the strain necessary for crystallization varies inversely with molecular weight because of relaxation. However, lower molecular weight PET might be expected to crystallize at a lower extent of molecular orientation, since the crystallization rate also varies inversely with molecular weight. Chain conformations were measured during low temperature drawing of PET of various molecular weights. The molecular configuration associated with strain induced crystallization was found to be independent of chain length. The onset of orientational crystallization was associated with a particular conformation, and this critical trans/gauche ratio was equivalent for PETs of various molecular weights. The drawing behavior is thus in accord with theory concerning the transition of flexible chain polymes from isotropy to an ordered state. This result is congruent with previous studies suggesting the presence of extended chain crystallinity in amorphous PET after low temperature drawing.

INTRODUCTION

The configurational differences between flexible chain and rigid rod polymers underlie their distinct crystallization behaviors. To minimize the excluded volume, rigid polymers spontaneously orient (1). Only minor longitudinal adjustments from within the nematic state are then necessary to bring the atoms into registry, giving rise to formation of extended chain crystallites (2, 3). The exceptional strength and stiffness of materials comprising rigid rod polymers result from the inherent connectivity of such a crystalline structure. The crystallization of flexible chain polymers, requiring large conformational rearrangements and a significant heat of fusion, is accompanied by extensive back-folding; consequently, the mechanical properties are limited by the absence of crystal phase continuity. The use of orientation to augment the performance of flexible chain polymers reduces the dimensional stability of such materials.

It has long been recognized that extended chain crystallization of flexible chain polymers is a potential route to higher performance materials (4-6).

The excess free energy of folded chain crystallization decreases with the degree of molecular extension, whereby back-folding becomes more difficult as a chain molecule is extended. At a sufficient degree of uncoiling, extended chain crystallization becomes favored (2, 3, 6-8).

Poly(ethylene terephthalate) is one of many polymers for which an improved combination of stiffness, strength, and dimensional stability would be technologically attractive. A variety of approaches has been explored toward this end, including high speed spinning (9-11), high pressure crystallization (12, 13), high pressure extrusion (14-16), high temperature crystallization (17), and zone annealing (18-21). Inferences regarding the morphology obtained by these methods typically rely on post-processing structural studies in combination with process and property correlations. At least some of these investigations have provided indications of extended chain crystallinity in the PET (9, 11, 12, 14-19).

From a fundamental viewpoint it is advantageous to employ a controllable process in attempting to assess the existence and nature of extended chain crystallization in flexible chain polymers. Because of its slow crystallization rate, PET can be quenched from above its melting point to below its glass

---

*Current address: Dow Chemical Research Center, Walnut Creek, Calif.

transition temperature to yield an amorphous, but highly crystallizable, material. The randomly coiled molecules can be subsequently extended mechanically at temperatures too low for normal (i.e., folded chain) crystallization. The "induced rigidity" effected by the stretching may engender extended chain crystallization in the manner of rigid rod polymers (2, 3, 6-8). From statistical mechanics considerations, predictions have been made concerning the degree of rigidity necessary to stabilize the nematic state (2, 3). At a given volume concentration, the axial ratio (or aspect ratio) of the molecules determines the relative stabilities of the isotropic and nematic phases. A discontinuous first order transition from complete isotropy to partial order is predicted with increase in axial ratio. This should be accompanied by a transition in the mode of crystallization from folded to fully chain extended.

Low temperature drawing experiments have been carried out extensively with PET. Although many of the resulting morphological features have been examined (16, 22-27), this information is not necessarily informative regarding the existence of an extended chain crystal structure. This is particularly true if substantial folded chain crystal overgrowth exists, such that the significance of average structural parameters is obscured. In this situation neither the crystal dimension along the chain axis, the fiber long period, nor the infrared fold band intensity can directly substantiate the existence of extended chain crystallinity.

When amorphous PET was uniaxially extended at room temperature (the glass transition temperature, T_g, equals 70°C), light scattering measurements indicated the presence of a "shish kebab" morphology, that is, an extended chain crystal core surrounded by folded chain lamellae (25). Such drawing conducted at slightly above T_g (but below the isotropic crystallization temperature), produces a fibrillar morphology superposed on a "rodlike superstructure," the latter aligned perpendicular to the stretching direction (25, 26). Although the greater degree of crystallinity at higher temperature masks the structural details, this behavior is consistent with models predicting orientational crystallization forming an extended chain framework, followed by development of folded chain overgrowth (28-30).

Drawing at slightly above T_g is the first step of the "zone annealing" method reported to produce PET fibers of high modulus (18-21). Elongation at 90°C of initially amorphous PET, followed by annealing at higher temperatures, produces fibers whose properties suggest the existence of fully extended chain crystals (18, 19). A similar process was utilized to produce PET fibers described as comprising extended chain crystals and having a remarkably high modulus (33 Gpa!) (31).

Although the results of these low temperature drawing experiments may imply extended chain crystallization of the PET, such conclusions are arguable. Alternative explanations for the structure

and properties have been proposed (23, 32). Low temperature drawing may simply produce conventional folded chain crystallization, transpiring at a greatly accelerated rate because of the orientation (33-35). The morphology of oriented semicrystalline PET is too complicated to allow definitive conclusions regarding this critical aspect of the structure. An alternative approach toward this problem is useful.

Molecular weight effects per se are secondary with regard to nematic behavior (36). In fact the formation of an ordered phase, with consequent extended chain crystallization, is predicted to transpire at a critical value of the chain axial ratio, independently of molecular weight (2, 3, 36). Conversely, if the low temperature drawing of PET is governed by the rate of folded chain crystallization, the strong dependence of crystallization rate on molecular weight (37, 38) would confer a molecular weight dependence to the process. The intention of the present study is to determine the conformational state associated with strain induced crystallization of PET. From the molecular weight dependence of this chain configuration, conformance to expectations for a liquid to nematic phase transition can be evaluated, and hence the probability of extended chain crystallization assessed.

EXPERIMENTAL

The additive-free PET was obtained from the Goodyear Tire and Rubber Co. The polymers had intrinsic viscosities (I.V.) of 0.59, 0.84, and 1.04 dl/g, respectively, which corresponds to a molecular weight range of 40,000 to 80,000. The PET was dried at 130°C in vacuum for 48 h, prior to being molded into films (50 μm thick) at 280°C under pressure. The films were quenched in an ice water bath to suppress crystallization. An absence of initial crystallinity was confirmed by wide angle X-ray scattering measurements, obtained using a Philips 2.5 kW generator with Cu target and Statton camera, and from the sample mass densities. The latter were measured in a density gradient column filled with carbon tetrachloride and ethanol.

The films, initially unoriented as inferred from a lack of birefringence, were uniaxially extended in an Instron 1135 at a nominal strain rate of 3×10^{-3} sec^{-1}. The drawing was conducted at 85°C, a temperature at which thermal (unoriented) crystallization is immeasurably slow. It has been shown that the strain induced crystallization behavior of PET is essentially independent of temperature over the range of 75 to 95°C (39). After drawing, test specimens were immediately removed from the environmental chamber and air cooled to room temperature. The strain was determined from fiducial marks.

FTIR measurements were made using a Perkin-Elmer 1800 spectrophotometer. Unpolarized spectra were obtained at 2 cm^{-1} resolution in single beam ratio mode. The spectra were analyzed by fitting Lorentzian profiles to the five absorption bands pres-

ent over the range of 930 to 760 cm^{-1} (40, 41). A representative IR spectrum and its nonlinear least squares best-fit curve are displayed in *Fig. 1*. The integral intensities obtained by curve fitting the overlapping bands are quantitatively different from band intensities estimated using the "pseudo-baseline" approximation (13, 41).

RESULTS

A simple comparison can be made between the equilibrium chain dimensions of PET and the critical value of the chain axial ratio below which configurational isotropy is favored. The minimum axial ratio for a stable nematic phase in a neat liquid is 6.7 (3). This can be compared to the axial ratio of a PET molecule, calculated as the ratio of its Kuhn segment length, l_k, to the chain diameter. The latter is given by

$$d = \sqrt{m/N\rho l} \qquad (1)$$

where m is the monomer unit molecular weight, ρ the mass density, and N is Avogadro's number. The mean square end-to-end distance for PET is

$$\langle r_0^2 \rangle_{PET} = 4.15 n l^2 \qquad (2)$$

where n ($= 6$) and l ($= 2.7$ Å) are, respectively, the number and average projection length of the virtual skeletal bonds (42). The Kuhn segment length must be consistent with both *Eq 2* and the length of a PET chain unit in the trans configuration, which is determined to be 10.9 Å. This yields $l_k = 16.2$ Å; hence the axial ratio

$$\frac{l_K}{d} = 3.5 \qquad (3)$$

is found to be less than 6.7. Theory correctly predicts the isotropy, and thus folded chain crystallinity, of unoriented PET.

When PET is drawn at 85°C the chain axial ratio assumes values higher than 3.5, and these are maintained while the polymer is below its glass transition temperature. The equilibrium configuration is at least partially recovered when the drawn film is subsequently exposed to temperatures above T_g (*Fig. 2*). Initially the shrinkage increases with strain, reflecting the greater molecular anisotropy. At higher strains, however, the shrinkage is reduced as development of a crystalline phase stabilizes the morphology. This effect has been used as a measure of the extent of crystallinity in PET (33).

As shown in *Fig. 3*, the density also increases during drawing, even at strains for which PET remains amorphous (as judged by X-ray scattering). The simple proportionality between the amorphous
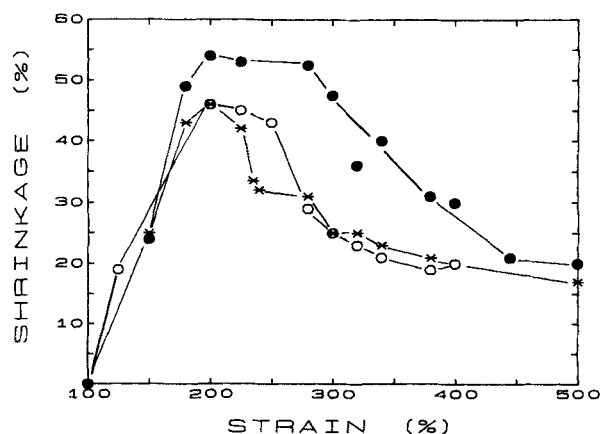
Fig. 2. The shrinkage measured after 85°C drawing of amorphous PET to various elongations (I.V. = 0.59 ●●●, 0.84 ○○○, and 1.04 ***, respectively).

Fig. 3. The mass density measured for PET films (I.V. = 0.59 ●●●, 0.84 ○○○, and 1.04 ***, respectively) drawn to the indicated strains at 85°C. The initial straight lines are least squares fits to the lower strain data. Orientational crystallization occasions the deviation from linearity. The intermediate I.V. film has an initially lower density due probably to the presence of voids.
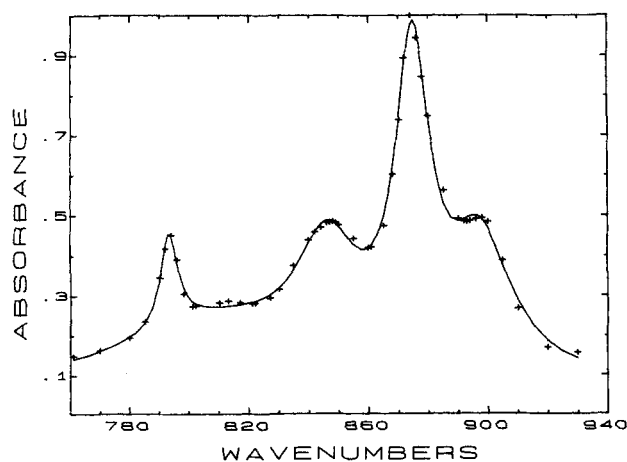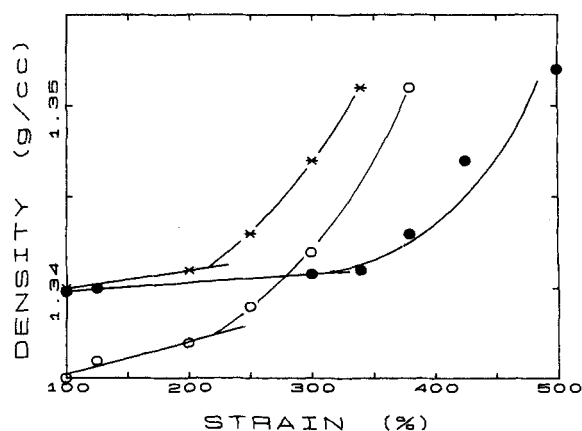

Fig. 1. The FTIR spectrum measured for an amorphous PET film (I.V. = 1.04) drawn to an extension ratio of 2. The curve is the best-fit calculation assuming Lorentzian line shapes. The trans and gauche bands used for determination of the rotameric composition are centered at 846 cm^{-1} and 898 cm^{-1} respectively.

density of PET and its orientation has been described previously (9). Strain induced crystallization causes an increase in slope of the density vs. strain relationship (*Fig. 3*).

The wide angle X-ray scattering from the PET after various extents of drawing are similar to previously reported results (16, 25, 26). The diffraction patterns reveal the development of significant order prior to the appearance of the sharp reflections associated with a crystalline state. The existence in stretched PET of a mesophase, described as a paracrystalline or highly oriented amorphous phase, has often been noted (16, 43–46). The transition from isotropy to a condition of partial order is predicted to be abrupt and discontinuous (3, 6, 7, 8). This ordered phase is responsible for the spontaneous onset of strain induced crystallization.

The chain extension effected by the drawing, however, is partially countervailed by relaxation. The lower molecular weight polymer relaxes faster at 85°C. This is a consequence not only of shorter chain length per se, but also of a slightly lower T_g (about 3° in going from an I.V. of 1.40 to an I.V. equal to 0.59). This influence of chain length on the degree of molecular extension attained at a given macroscopic extension is illustrated in *Fig. 4*. During stretching of the PET the population of trans conformers is seen to increase relative to that of the gauche rotamers; however, the effect is amplified at higher molecular weights. Accordingly, orientational crystallization in the lower molecular weight PET requires higher levels of macroscopic strain. A decrease in shrinkage measured for the film (*Fig. 2*) and a marked increase in density with strain (*Fig. 3*) both reflect the onset of crystallization. These occur at higher macroscopic strain in the lower molecular weight PET.

Of primary interest here is the molecular conformation associated with the onset of crystallization. The onset of crystallization was determined from *Fig. 2* as the strain associated with a marked decrease in shrinkage. This point was particularly evident in derivative curves (not shown) for the data. The strain at which crystallization commences was also deduced from the density measurements in *Fig. 3*. The density of amorphous PET is a linear function of the amorphous orientation (9); the deviation from linearity provides an indication of the onset of crystallization.

Although this crystallization is manifested in the shrinkage and density of the drawn films, the relationship of these quantities to crystallinity is complex. In this regard, it is noted that the degree of crystallinity in PET varies widely as measured by density, X-ray, calorimetry, and NMR (45). While a determination can be made of the strain at which crystallization is induced from either shrinkage and density measurements, equivalent results from these two methods are neither expected nor obtained. Nevertheless, either determination enables the conformation of the PET associated with the

inducement of crystallization to be ascertained. Using *Fig. 4*, the relative intensities of the trans and gauche absorption bands at the macroscopic strain identified with the onset of strain induced crystallization could be determined. These numbers, which are proportional to the respective rotameric state populations, are listed in *Table 1*.

It is seen that within the experimental error, there is no dependence on molecular weight in the degree of chain extension necessary to effect crystallization by low temperature drawing.

This equivalency for various molecular weights of the chain conformation at the onset of crystallization conforms to the predictions of polymer liquid crystal theory (2, 3). The induced rigidity of the PET confers a larger axial ratio. When the molecular extension exceeds a critical value [equal to 6.7 in the Flory model (3)], nematic phase behavior prevails and thus governs the crystallization process. The orientational crystallization behavior is consistent with the formation of extended chain crystallites.

As noted above, the rate of normal (i.e., folded chain) crystallization increases with molecular orientation, although in PET the effect is reduced at temperatures in the vicinity of the drawing temperature used herein (34, 35). Once crystallization, os-
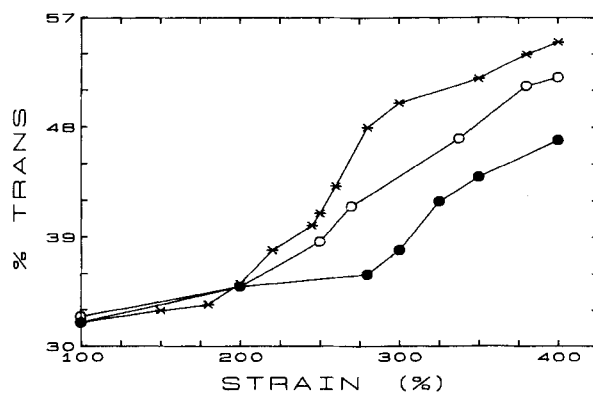

Fig. 4. *The intensity of the trans absorption band at 846 cm^{-1} divided by the sum of the intensities of the trans and the gauche band (at 898 cm^{-1}) for PET drawn to various strains. The integral intensities were calculated from the Lorentzian profiles obtained by fitting the measured FTIR spectra (see Fig. 1). The symbols are as defined for Figs. 2 and 3.*

Table 1. Rotameric Population at Onset of Crystallization.

Determination[b]	Relative Trans Absorption (%)[a]		
	0.59[c]	0.84[c]	1.04[c]
Shrinkage	36	39	35
Density	40	37	38

[a]Integral area of trans absorption peak (at 846 cm^{-1}) divided by sum of integral intensities of trans and gauche absorption bands (the latter at 898 cm^{-1}), measured at the strain associated with the onset of crystallization. The intensities are obtained by fitting Lorentzian functions to the overlapping bands.
[b]Method used to ascertain the onset of orientational crystallization.
[c]Intrinsic viscosity in dl/g.

tensibly in the extended chain configuration, commences, an ensuing development of substantial folded chain crystalline overgrowth is expected if sufficient temperatures are maintained (19, 24, 28–30). In the infrared spectra for the drawn films there was no observable absorption at 988 cm^{-1} attributable to the fold conformation (47). This is at least consistent with extended chain crystallinity.

The crystallization rate also increases inversely with molecular weight. This is a consequence of enhanced mobility, which is directly reflected in the faster relaxation of the lower molecular weight PET seen in *Fig. 4*. If the strain induced crystallization observed here were attributable to an orientational enhancement of the folded chain crystallization rate, the lower I.V. PET would crystallize more readily. Crystallization would transpire at a lower extent of molecular orientation (although, because of relaxation, this might require a larger macroscopic strain). Contrarily, and hence incongruent with the onset of folded chain crystallization, the molecular configuration associated with strain induced crystallization is found to be independent of molecular weight.

A direct comparison of the experimentally measured chain conformation upon crystallization to the predicted level of trans rotamers necessary for rigid rod behavior [37% according to the Flory theory (2, 3)] is unwarranted given the approximate nature of the model. The Flory value was deduced by assuming an idealized chain on a cubic lattice, and thus provides a crude description of rods in the nematic state (2).

SUMMARY

Results of previous studies on the low temperature drawing of PET have been reconciled by the suggestion that an intermediate, highly ordered amorphous phase exists. The premise of a liquid crystalline phase transition is supported by the present finding that the molecular conformation associated with the onset of crystallinity during low temperature drawing is independent of chain length. This invariance to molecular weight is inconsistent with a simple orientation-enhancement of the crystallization rate, for which a higher degree of molecular extension would be expected for the higher I.V. PET (given its slower crystallization rate). The highly oriented mesophase serves as the precursor for extended chain crystallization. Orientation prior to crystallization is the prerequisite for suppression of the backfolding that normally accompanies crystallization of flexible chain polymers.

The slow, low temperature drawing experiments described here illustrate the concept of extended chain crystallization of flexible chain polymers; however, the higher deformation rates of more practical processes may cause departures due to nonequilibrium effects. Notwithstanding this possibility, high speed fiber spinning (9–11), zone annealing (18, 19), and high pressure extrusion (14–16)

technologies likely represent actual implementations of the phenomenon.

REFERENCES

1. L. Onsager, *Ann. N.Y. Acad. Sci.*, **51**, 627 (1949).
2. P. J. Flory, *Proc. R. Soc. Lond.*, A234, 60 (1956).
3. P. J. Flory, *Adv. Polym. Sci.*, **59**, 1 (1984).
4. F. C. Frank, *Proc. R. Soc. Lond.* A319, 127 (1970).
5. D. M. Bigg, *Polym. Eng. Sci.*, **16**, 725 (1976).
6. S. Frenkel, *J. Polym. Sci. Polym. Symp.*, **58**, 195 (1977).
7. G. K. Elyashevich, V. G. Baranov, and S. Y. Frenkel, *J. Macro. Sci. Phys.*, B13, 255 (1977).
8. G. K. Elyashevich, *Adv. Polym. Sci.*, **43**, 205 (1982).
9. H. M. Heuvel and R. Huisman, *J. Appl. Polym. Sci.*, **22**, 2229 (1978).
10. P. Desai and A. S. Abhiraman, *J. Polym. Sci., Polym. Phys. Ed.*, **26**, 1657 (1988).
11. H. A. Hristov and J. M. Schultz, *J. Polym. Sci. Polym. Phys. Ed.*, **28**, 1647 (1990).
12. A. Siegmann and P. J. Harget, *J. Polym. Sci. Polym. Phys. Ed.*, **18**, 2181 (1980).
13. P. J. Phillips and H. T. Tseng, *Macromolecules*, **22**, 1649 (1989).
14. P. D. Griswold and J. A. Cuculo, *J. Appl. Polym. Sci.*, **22**, 163 (1978).
15. J. R .C. Pereira and R. S. Porter, *J. Polym. Sci. Polym. Phys. Ed.*, **21**, 1133 (1983).
16. T. Sun, A. Zhang, F. M. Li, and R. S. Porter, *Polymer*, **29**, 2115 (1988).
17. C. M. Roland, *Polym. Eng. Sci.*, **31**, 849 (1991).
18. T. Kunugi, A. Suzuki, and M. Hashimoto, *J. Appl. Polym. Sci.*, **26**, 213 (1981).
19. T. Kunugi, C. Ichinose, and A. Suzuki, *J. Appl. Polym. Sci.*, **31**, 429 (1986).
20. G. Hinrichsen, P. Wolbring, and H. Springer, in *Interrelations Between Processing, Structure, and Properties of Polymeric Materials*, J. C. Seferis, and P. S. Theocaris, eds., Elsevier, Amsterdam (1984).
21. D. Hofmann, U. Goschel, E. Walenta, D. Geiss, and B. Philipp, *Polymer*, **30**, 242 (1989).
22. S. R. Padibjo and I. M. Ward, *Polymer*, **24**, 1103 (1983).
23. S. Fakirov and M. Evstatiev, *Polymer*, **31**, 431 (1990).
24. G. le Bourvellec, L. Monnerie, and J. P. Jarry, *Polymer*, **28**, 1712 (1987).
25. A. Misra and R. S. Stein, *J. Polym. Sci. Polym. Phys. Ed.*, **17**, 235 (1979).
26. M. Matsuo, M. Tamada, T. Terada, C. Sawatari, and M. Niwa, *Macromolecules*, **15**, 988 (1982).
27. T. Thistlethwaite, R. Jakeways, and I. M. Ward, *Polymer*, **29**, 61 (1988).
28. A. Keller and M. R. Mackley, *Pure Appl. Chem.*, **39**, 195 (1974).
29. A. Peterlin, *Polym. Eng. Sci.*, **16**, 126 (1976).
30. R. J. Gaylord and D. J. Lohse, *Polym. Eng. Sci.*, **16**, 163 (1976).
31. V. V. Krenev, M. I. Simonova, E. M. Aizenshtein, V. G. Baranov, and S. Y. Frenkel, *Fiber Chem.*, **1**, 53 (1978).
32. G. S. Y. Yeh, *Polym. Eng. Sci.*, **16**, 145 (1976).
33. F. S. Smith and R. D. Steward, *Polymer*, **15**, 284 (1974).

34. G. C. Alfonso, M. P. Verdona, and A. Wasiak, *Polymer*, **19**, 711 (1978).
35. G. Althen and H. G. Zachmann, *Makromol. Chem.*, **180**, 2723 (1979).
36. P. J. Flory, *Macromolecules*, **11**, 1141 (1978).
37. F. van Antwerpen and D. W. van Krevelen, *J. Polym. Sci.*, **10**, 2423 (1972).
38. B. Gumther, and H. G. Zachmann, *Polymer*, **24**, 1008 (1983).
39. G. P. Andrianova, Y. V. Popov, S. D. Artamonova, and B. A. Arutyunov, *Polym. Sci. U.S.S.R.*, **19**, 1418 (1977).
40. A. Miyake, *J. Polym. Sci.*, **38**, 479 (1959).
41. A. Cunningham, I. M. Ward, H. A. Willis, and V. Zichy, *Polymer*, **15**, 749 (1974).
42. A. D. Williams and P. J. Flory, *J. Polym. Sci.*, **5**, 417 (1967).
43. D. C. Prevorsek, *J. Polym. Sci.*, **32**, 343 (1971).
44. T. Asano, and T. Seto, *Polym. J.*, **5**, 72 (1973).
45. J. R. Havens and D. L. VanderHart, *Macromolecules*, **18**, 1663 (1985).
46. D. L. Tzou, P. Desai, A. S. Abhiraman, and T.-H. Huang, *J. Polym .Sci. Polym. Phys. Ed.*, **29**, 49 (1991).
47. J. L. Koenig and M. J. Hannon, *J. Macro. Sci. Phys.* **B1**, 119 (1967).